

NOTE: THE FIGURES IN THIS SECTION ARE INTENDED TO SHOW THE REPRESENTATIVE DATA. THEY ARE NOT MEANT TO BE COMPLETE COMPILATIONS OF ALL THE WORLD'S RELIABLE DATA.

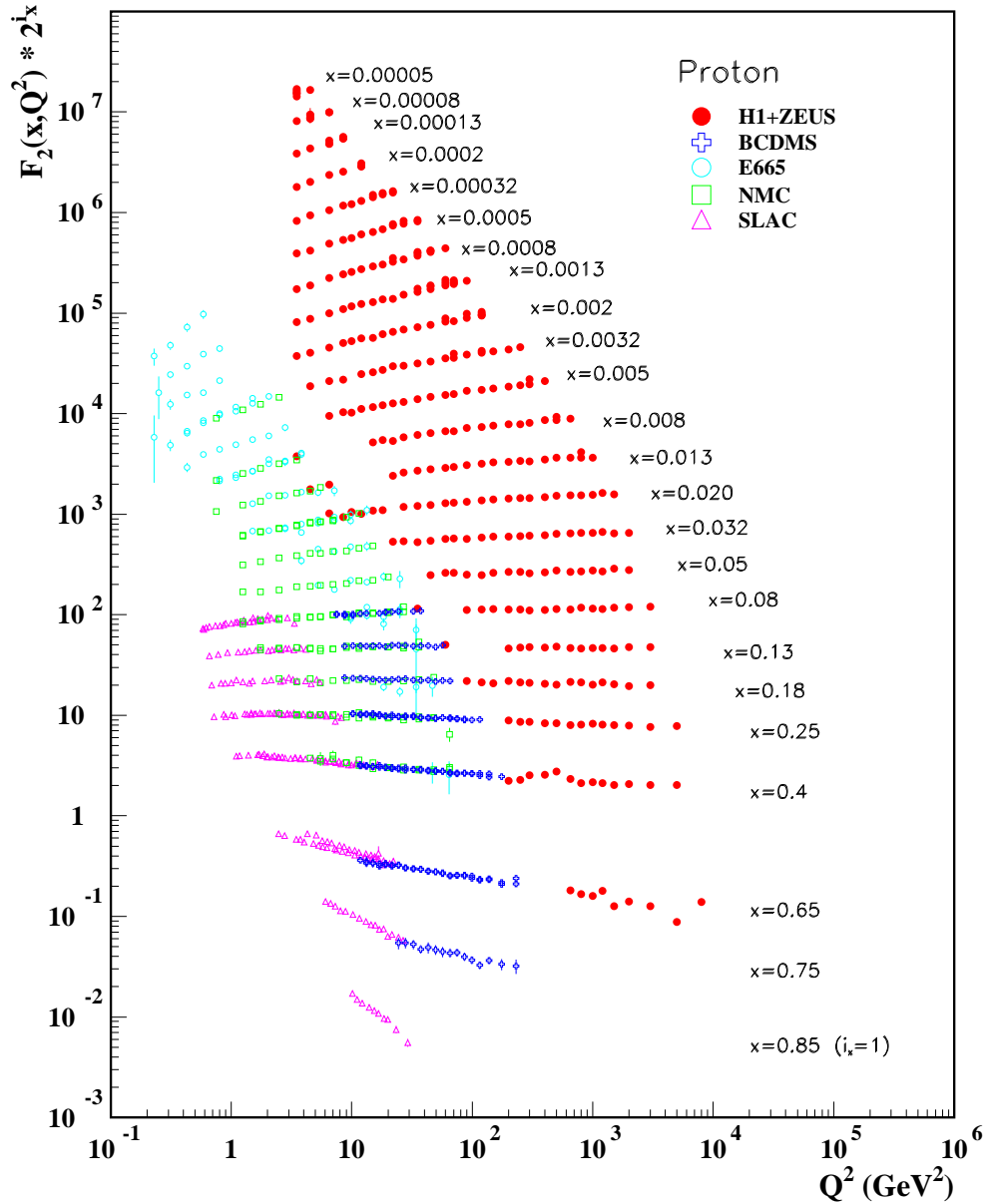


Figure 18.8: The proton structure function F_2^p measured in electromagnetic scattering of electrons and positrons on protons (collider experiments H1 and ZEUS for $Q^2 \geq 2 \text{ GeV}^2$), in the kinematic domain of the HERA data (see Fig. 18.10 for data at smaller x and Q^2), and for electrons (SLAC) and muons (BCDMS, E665, NMC) on a fixed target. Statistical and systematic errors added in quadrature are shown. The H1+ZEUS combined values are obtained from the measured reduced cross section and converted to F_2^p with a HERAPDF NLO fit, for all measured points where the predicted ratio of F_2^p to reduced cross-section was within 10% of unity. The data are plotted as a function of Q^2 in bins of fixed x . Some points have been slightly offset in Q^2 for clarity. The H1+ZEUS combined binning in x is used in this plot; all other data are rebinned to the x values of these data. For the purpose of plotting, F_2^p has been multiplied by 2^{i_x} , where i_x is the number of the x bin, ranging from $i_x = 1$ ($x = 0.85$) to $i_x = 24$ ($x = 0.00005$). References: **H1 and ZEUS**—H. Abramowicz *et al.*, Eur. Phys. J. **C75**, 580 (2015) (for both data and HERAPDF parameterization); **BCDMS**—A.C. Benvenuti *et al.*, Phys. Lett. **B223**, 485 (1989) (as given in [86]); **E665**—M.R. Adams *et al.*, Phys. Rev. **D54**, 3006 (1996); **NMC**—M. Arneodo *et al.*, Nucl. Phys. **B483**, 3 (1997); **SLAC**—L.W. Whitlow *et al.*, Phys. Lett. **B282**, 475 (1992).

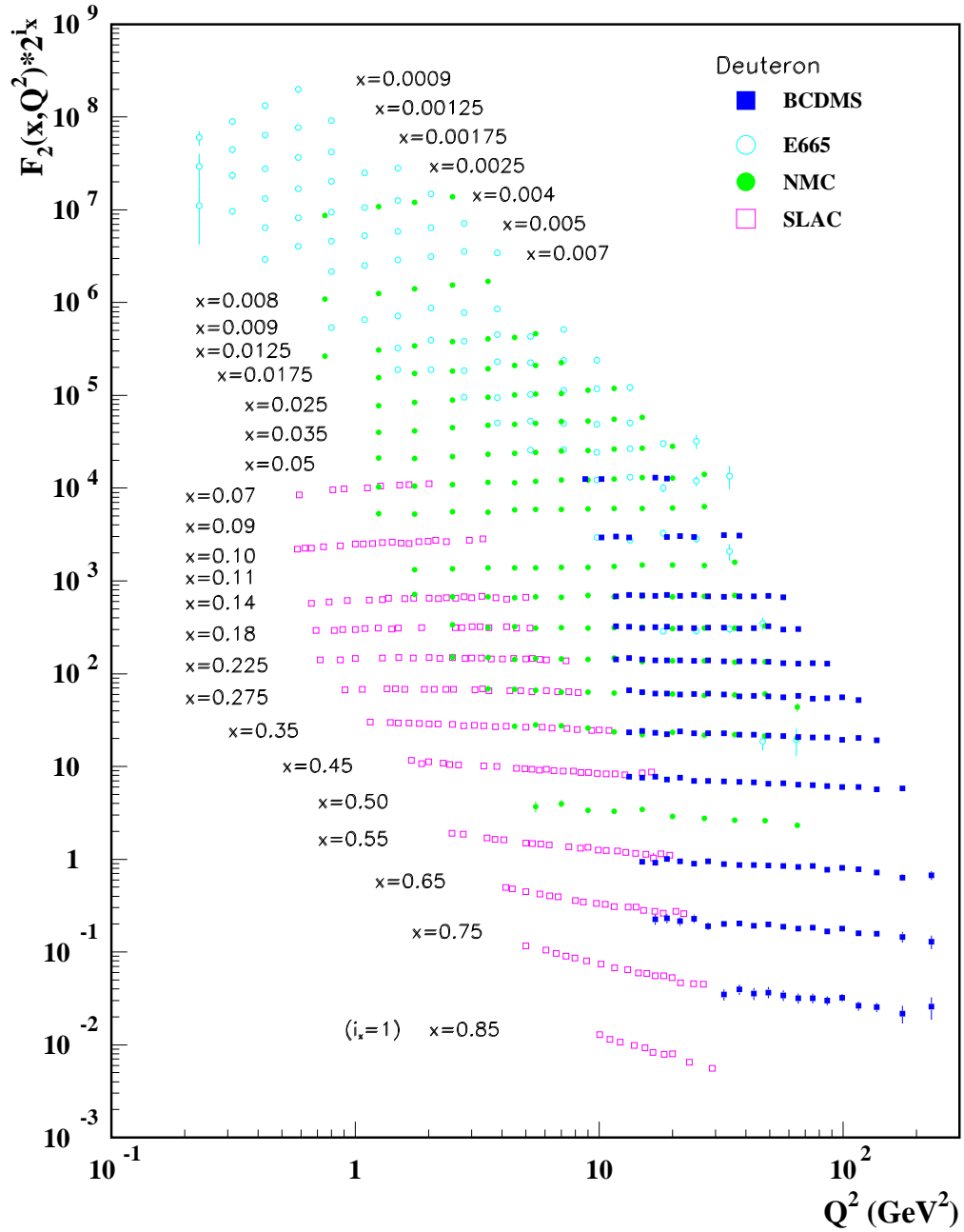


Figure 18.9: The deuteron structure function F_2^d measured in electromagnetic scattering of electrons (SLAC) and muons (BCDMS, E665, NMC) on a fixed target, shown as a function of Q^2 for bins of fixed x . Statistical and systematic errors added in quadrature are shown. For the purpose of plotting, F_2^d has been multiplied by 2^{i_x} , where i_x is the number of the x bin, ranging from 1 ($x = 0.85$) to 29 ($x = 0.0009$). References: **BCDMS**—A.C. Benvenuti *et al.*, Phys. Lett. **B237**, 592 (1990). **E665, NMC, SLAC**—same references as Fig. 18.8.

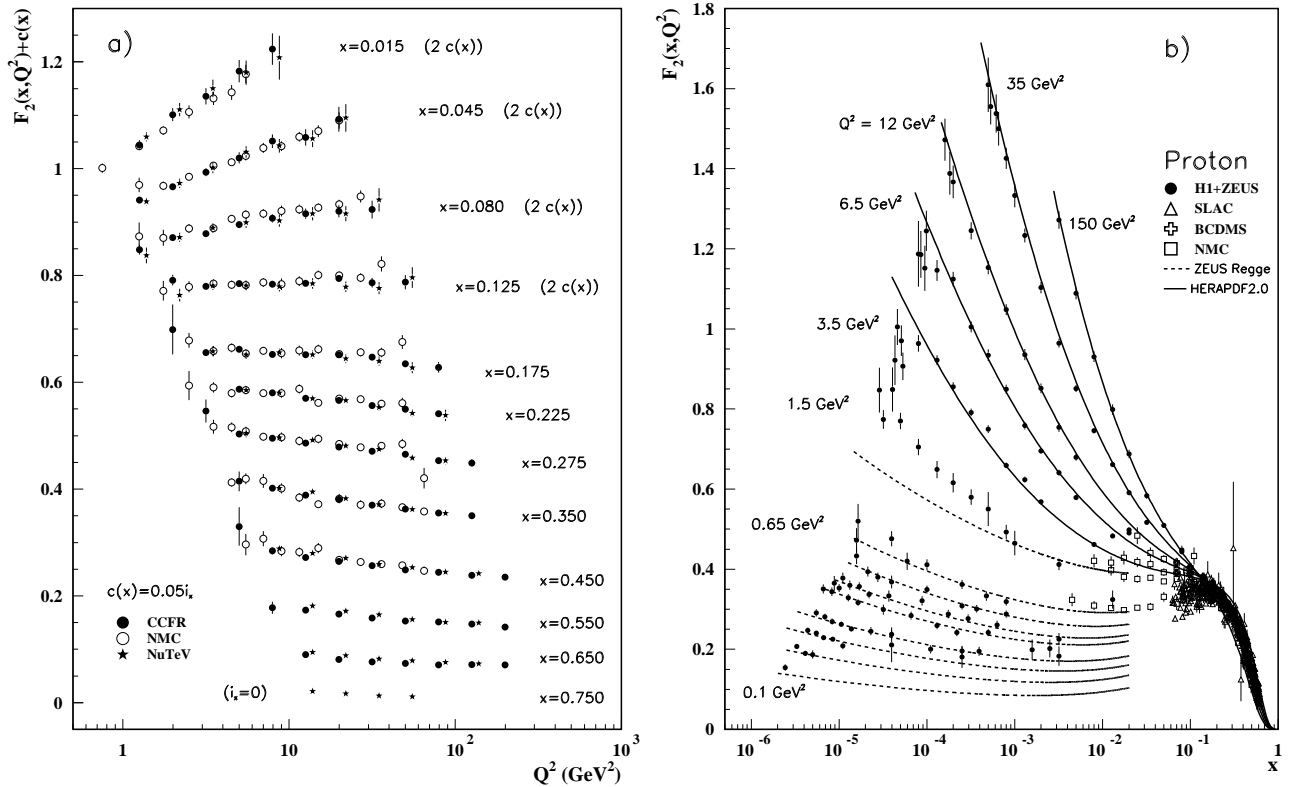


Figure 18.10: a) The deuteron structure function F_2 measured in deep inelastic scattering of muons on a fixed target (NMC) is compared to the structure function F_2 from neutrino-iron scattering (CCFR and NuTeV) using $F_2^\mu = (5/18)F_2^\nu - x(s + \bar{s})/6$, where heavy-target effects have been taken into account. The data are shown versus Q^2 , for bins of fixed x . The NMC data have been rebinned to CCFR and NuTeV x values. For the purpose of plotting, a constant $c(x) = 0.05i_x$ is added to F_2 , where i_x is the number of the x bin, ranging from 0 ($x = 0.75$) to 7 ($x = 0.175$). For $i_x = 8$ ($x = 0.125$) to 11 ($x = 0.015$), $2c(x)$ has been added. References: **NMC**—M. Arneodo *et al.*, Nucl. Phys. **B483**, 3 (1997); **CCFR/NuTeV**—U.K. Yang *et al.*, Phys. Rev. Lett. **86**, 2741 (2001); **NuTeV**—M. Tzanov *et al.*, Phys. Rev. **D74**, 012008 (2006).

b) The proton structure function F_2^p mostly at small x and Q^2 , measured in electromagnetic scattering of electrons and positrons (H1, ZEUS), electrons (SLAC), and muons (BCDMS, NMC) on protons. Lines are ZEUS Regge and HERAPDF parameterizations for lower and higher Q^2 , respectively. The width of the bins can be up to 10% of the stated Q^2 . Some points have been slightly offset in x for clarity. The H1+ZEUS combined values for $Q^2 \geq 3.5$ GeV² are obtained from the measured reduced cross section and converted to F_2^p with a HERAPDF NLO fit, for all measured points where the predicted ratio of F_2^p to reduced cross-section was within 10% of unity. A turn-over is visible in the low- x points at medium Q^2 (3.5 GeV² and 6 GeV²) for the H1+ZEUS combined values. In order to obtain F_2^p from the measured reduced cross-section, F_L must be estimated; for the points shown, this estimate is obtained from HERAPDF2.0. No F_L value consistent with the HERA data can eliminate the turn-over. This may indicate that at low x and Q^2 there are contributions to the structure functions that cannot be described in standard DGLAP evolution.

References: **H1 and ZEUS**—F.D. Aaron *et al.*, JHEP **1001**, 109 (2010) (data for $Q^2 < 3.5$ GeV²), H. Abramowicz *et al.*, Eur. Phys. J. **C75**, 580 (2015) (data for $Q^2 \geq 3.5$ GeV² and HERAPDF parameterization); **ZEUS**—J. Breitweg *et al.*, Phys. Lett. **B487**, 53 (2000) (ZEUS Regge parameterization); **BCDMS, NMC, SLAC**—same references as Fig. 18.8.

Statistical and systematic errors added in quadrature are shown for both plots.

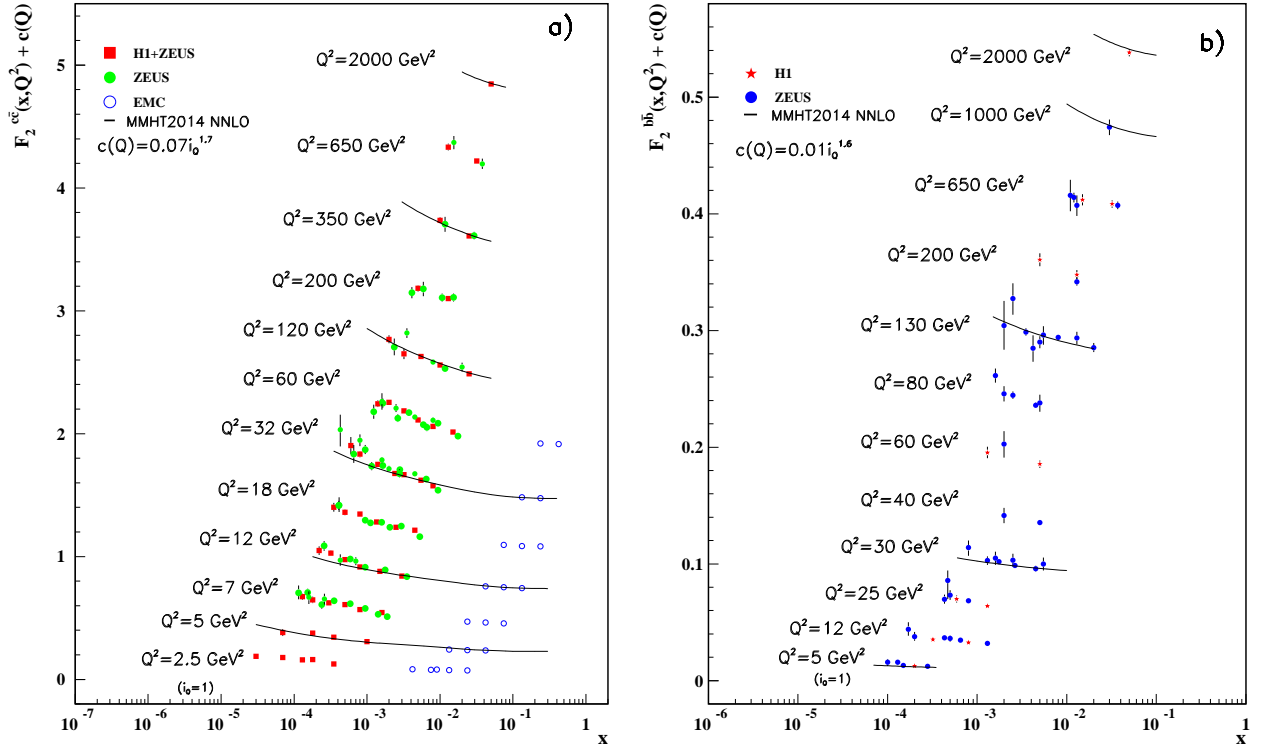


Figure 18.11: a) The charm-quark structure function $F_2^{c\bar{c}}(x)$, i.e. that part of the inclusive structure function F_2^p arising from the production of charm quarks, measured in electromagnetic scattering of positrons on protons (H1, ZEUS) and muons on iron (EMC). For the purpose of plotting, a constant $c(Q) = 0.07i_Q^{1.7}$ is added to $F_2^{c\bar{c}}$ where i_Q is the number of the Q^2 bin, ranging from 1 ($Q^2 = 2.5 \text{ GeV}^2$) to 12 ($Q^2 = 2000 \text{ GeV}^2$). References: **H1 and ZEUS run I combination**—H. Abramowicz *et al.*, Eur. Phys. J. **C73**, 2311 (2013); **ZEUS run II**—H. Abramowicz *et al.*, JHEP **05**, 023 (2013); H. Abramowicz *et al.*, JHEP **05**, 097 (2013); H. Abramowicz *et al.*, JHEP **09**, 127 (2014); **EMC**—J.J. Aubert *et al.*, Nucl. Phys. **B213**, 31 (1983).

b) The bottom-quark structure function $F_2^{b\bar{b}}(x)$. For the purpose of plotting, a constant $c(Q) = 0.01i_Q^{1.6}$ is added to $F_2^{b\bar{b}}$ where i_Q is the number of the Q^2 bin, ranging from 1 ($Q^2 = 5 \text{ GeV}^2$) to 12 ($Q^2 = 2000 \text{ GeV}^2$). References: **ZEUS**—S. Chekanov *et al.*, Eur. Phys. J. **C65**, 65 (2010); H. Abramowicz *et al.*, Eur. Phys. J. **C69**, 347 (2010); H. Abramowicz *et al.*, Eur. Phys. J. **C71**, 1573 (2011); H. Abramowicz *et al.*, JHEP **09**, 127 (2014); **H1**—F.D. Aaron *et al.*, Eur. Phys. J. **C65**, 89 (2010).

For both plots, statistical and systematic errors added in quadrature are shown. The data are given as a function of x in bins of Q^2 . Points may have been slightly offset in x for clarity. Some data have been rebinned to common Q^2 values. Also shown is the MMHT2014 parameterization given at several Q^2 values (L. A. Harland-Lang *et al.*, Eur. Phys. J. **C75**, 204 (2015)).

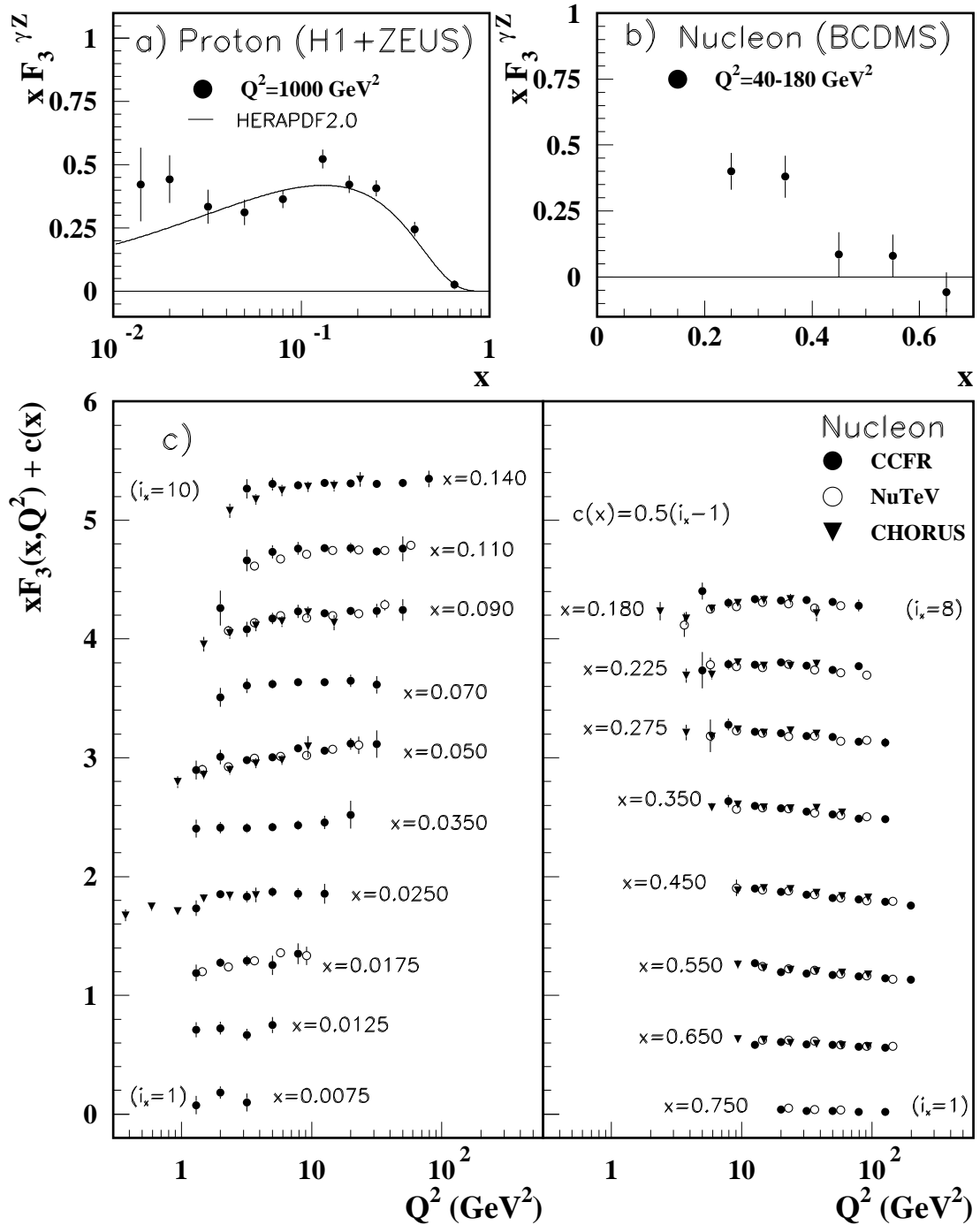


Figure 18.12: The structure function $x F_3^{\gamma Z}$ measured in electroweak scattering of **a)** electrons on protons (H1 and ZEUS) and **b)** muons on carbon (BCDMS). The line in **a)** is the HERAPDF parameterization. References: **H1 and ZEUS**—H. Abramowicz *et al.*, *Eur. Phys. J.* **C75**, 580 (2015) (for both data and HERAPDF parameterization); **BCDMS**—A. Argento *et al.*, *Phys. Lett.* **B140**, 142 (1984).

c) The structure function $x F_3$ of the nucleon measured in ν -Fe scattering. The data are plotted as a function of Q^2 in bins of fixed x . For the purpose of plotting, a constant $c(x) = 0.5(i_x - 1)$ is added to $x F_3$, where i_x is the number of the x bin as shown in the plot. The NuTeV and CHORUS points have been shifted to the nearest corresponding x bin as given in the plot and slightly offset in Q^2 for clarity. References: **CCFR**—W.G. Seligman *et al.*, *Phys. Rev. Lett.* **79**, 1213 (1997); **NuTeV**—M. Tzanov *et al.*, *Phys. Rev.* **D74**, 012008 (2006); **CHORUS**—G. Önençüt *et al.*, *Phys. Lett.* **B632**, 65 (2006).

Statistical and systematic errors added in quadrature are shown for all plots.

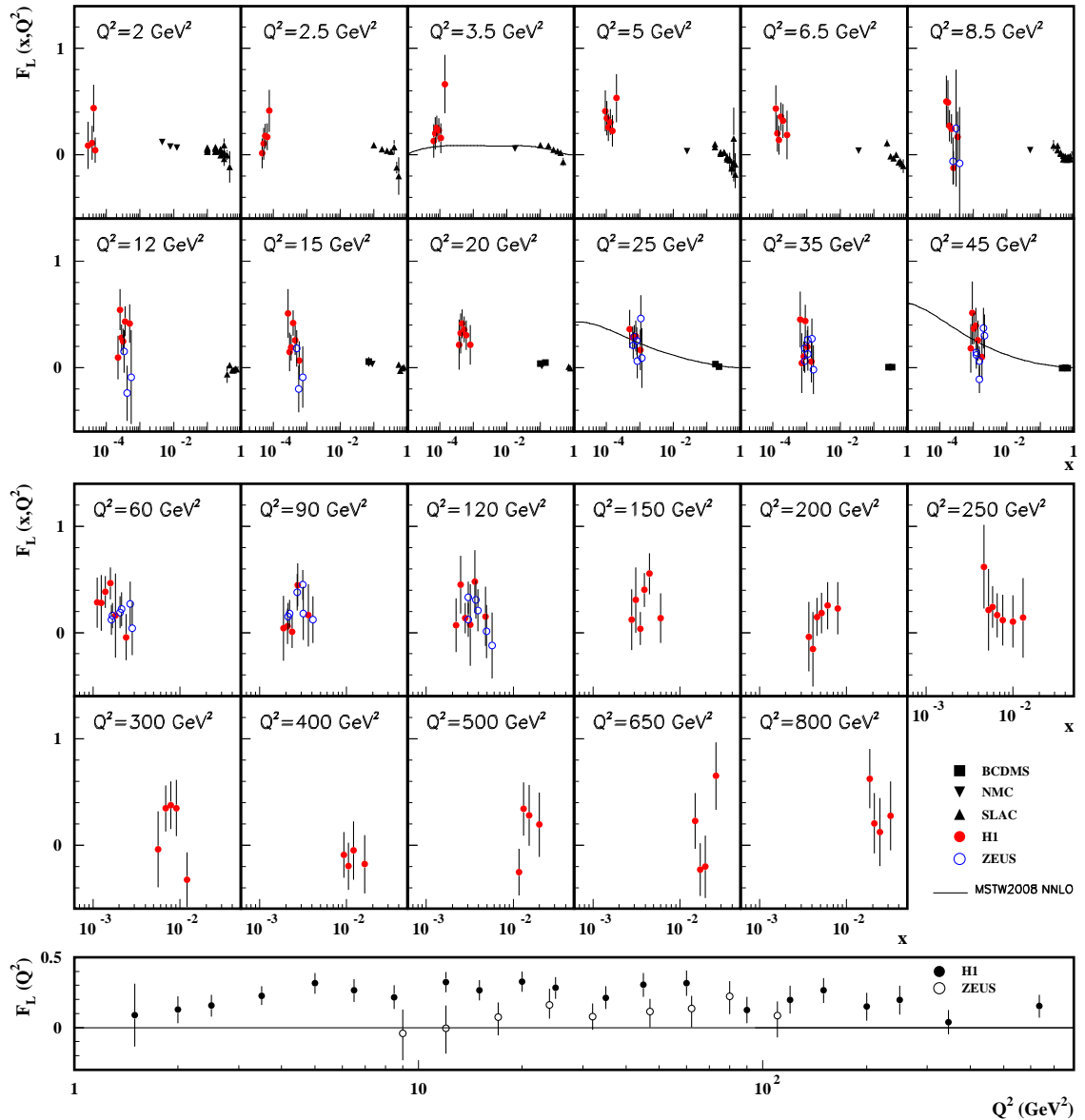


Figure 18.13: Top panels: The longitudinal structure function F_L as a function of x in bins of fixed Q^2 measured on the proton (except for the SLAC data which also contain deuterium data). BCDMS, NMC, and SLAC results are from measurements of R (the ratio of longitudinal to transverse photon absorption cross sections) which are converted to F_L by using the BDCMS parameterization of F_2 (A.C. Benvenuti *et al.*, Phys. Lett. **B223**, 485 (1989)). It is assumed that the Q^2 dependence of the fixed-target data is small within a given Q^2 bin. Some of the other data may have been rebinned to common Q^2 values. Some points have been slightly offset in x for clarity. Also shown is the MSTW2008 parameterization given at three Q^2 values (A.D. Martin *et al.*, Eur. Phys. J. **C63**, 189 (2009)). References: **H1**—V. Andreev *et al.*, Eur. Phys. J. **C74**, 2814 (2014); **ZEUS**—S. Chekanov *et al.*, Phys. Lett. **B682**, 8 (2009); H. Abramowicz *et al.*, Phys. Rev. **D90**, 072002 (2014); **BCDMS**—A. Benvenuti *et al.*, Phys. Lett. **B223**, 485 (1989); **NMC**—M. Arneodo *et al.*, Nucl. Phys. **B483**, 3 (1997); **SLAC**—L.W. Whitlow *et al.*, Phys. Lett. **B250**, 193 (1990) and numerical values from the thesis of L.W. Whitlow (SLAC-357).

Bottom panel: The longitudinal structure function F_L as a function of Q^2 . Some points have been slightly offset in Q^2 for clarity. References: **H1**—V. Andreev *et al.*, Eur. Phys. J. **C74**, 2814 (2014); **ZEUS**—H. Abramowicz *et al.*, Phys. Rev. **D90**, 072002 (2014).

The results shown in the bottom plot require the assumption of the validity of the QCD form for the F_2 structure function in order to extract F_L . Statistical and systematic errors added in quadrature are shown for both plots.

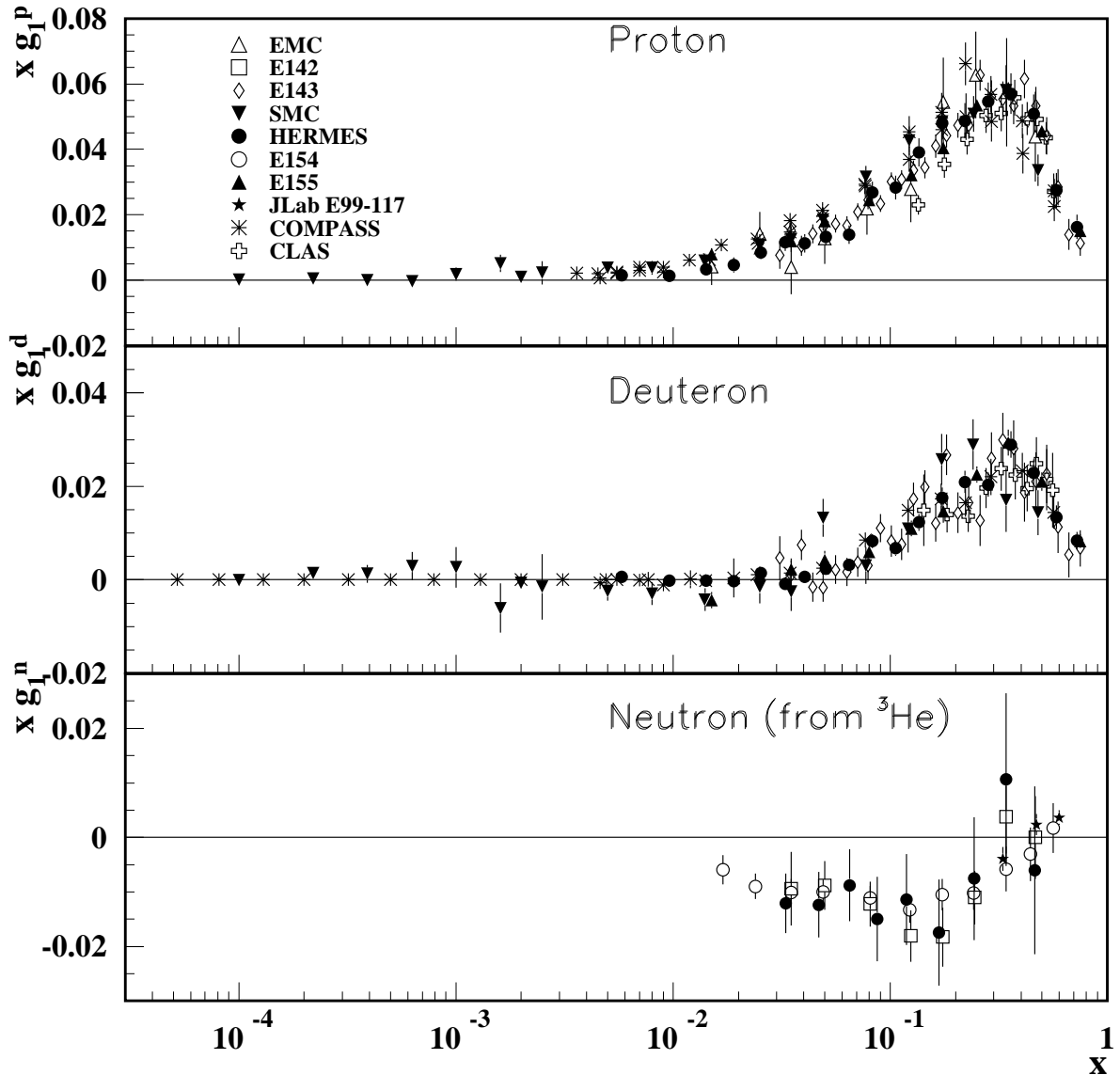


Figure 18.14: The spin-dependent structure function $xg_1(x)$ of the proton, deuteron, and neutron (from ^3He target) measured in deep inelastic scattering of polarized electrons/positrons: E142 ($Q^2 \sim 0.3 - 10 \text{ GeV}^2$), E143 ($Q^2 \sim 0.3 - 10 \text{ GeV}^2$), E154 ($Q^2 \sim 1 - 17 \text{ GeV}^2$), E155 ($Q^2 \sim 1 - 40 \text{ GeV}^2$), JLab E99-117 ($Q^2 \sim 2.71 - 4.83 \text{ GeV}^2$), HERMES ($Q^2 \sim 0.18 - 20 \text{ GeV}^2$), CLAS ($Q^2 \sim 1 - 5 \text{ GeV}^2$) and muons: EMC ($Q^2 \sim 1.5 - 100 \text{ GeV}^2$), SMC ($Q^2 \sim 0.01 - 100 \text{ GeV}^2$), COMPASS ($Q^2 \sim 0.001 - 100 \text{ GeV}^2$), shown at the measured Q^2 (except for EMC data given at $Q^2 = 10.7 \text{ GeV}^2$ and E155 data given at $Q^2 = 5 \text{ GeV}^2$). Note that $g_1^n(x)$ may also be extracted by taking the difference between $g_1^d(x)$ and $g_1^p(x)$, but these values have been omitted in the bottom plot for clarity. Statistical and systematic errors added in quadrature are shown. References: **EMC**—J. Ashman *et al.*, Nucl. Phys. **B328**, 1 (1989); **E142**—P.L. Anthony *et al.*, Phys. Rev. **D54**, 6620 (1996); **E143**—K. Abe *et al.*, Phys. Rev. **D58**, 112003 (1998); **SMC**—B. Adeva *et al.*, Phys. Rev. **D58**, 112001 (1998), B. Adeva *et al.*, Phys. Rev. **D60**, 072004 (1999) and Erratum-Phys. Rev. **D62**, 079902 (2000); **HERMES**—A. Airapetian *et al.*, Phys. Rev. **D75**, 012007 (2007) and K. Ackerstaff *et al.*, Phys. Lett. **B404**, 383 (1997); **E154**—K. Abe *et al.*, Phys. Rev. Lett. **79**, 26 (1997); **E155**—P.L. Anthony *et al.*, Phys. Lett. **B463**, 339 (1999) and P.L. Anthony *et al.*, Phys. Lett. **B493**, 19 (2000); **Jlab-E99-117**—X. Zheng *et al.*, Phys. Rev. **C70**, 065207 (2004); **COMPASS**—E.S. Ageev *et al.*, Phys. Lett. **B647**, 330 (2007), M.G. Alekseev *et al.*, Phys. Lett. **B690**, 466 (2010), C. Adolph, *et al.*, Phys. Lett. **B753**, 18 (2016) and C. Adolph, *et al.*, Phys. Lett. **B769**, 34 (2017); **CLAS**—K.V. Dharmawardane *et al.*, Phys. Lett. **B641**, 11 (2007) (which also includes resonance region data not shown on this plot — there is also low W^2 CLAS data in Y. Prok *et al.*, Phys. Rev. **C90**, 025212 (2014) and N. Guler *et al.*, Phys. Rev. **C92**, 055201 (2015)).

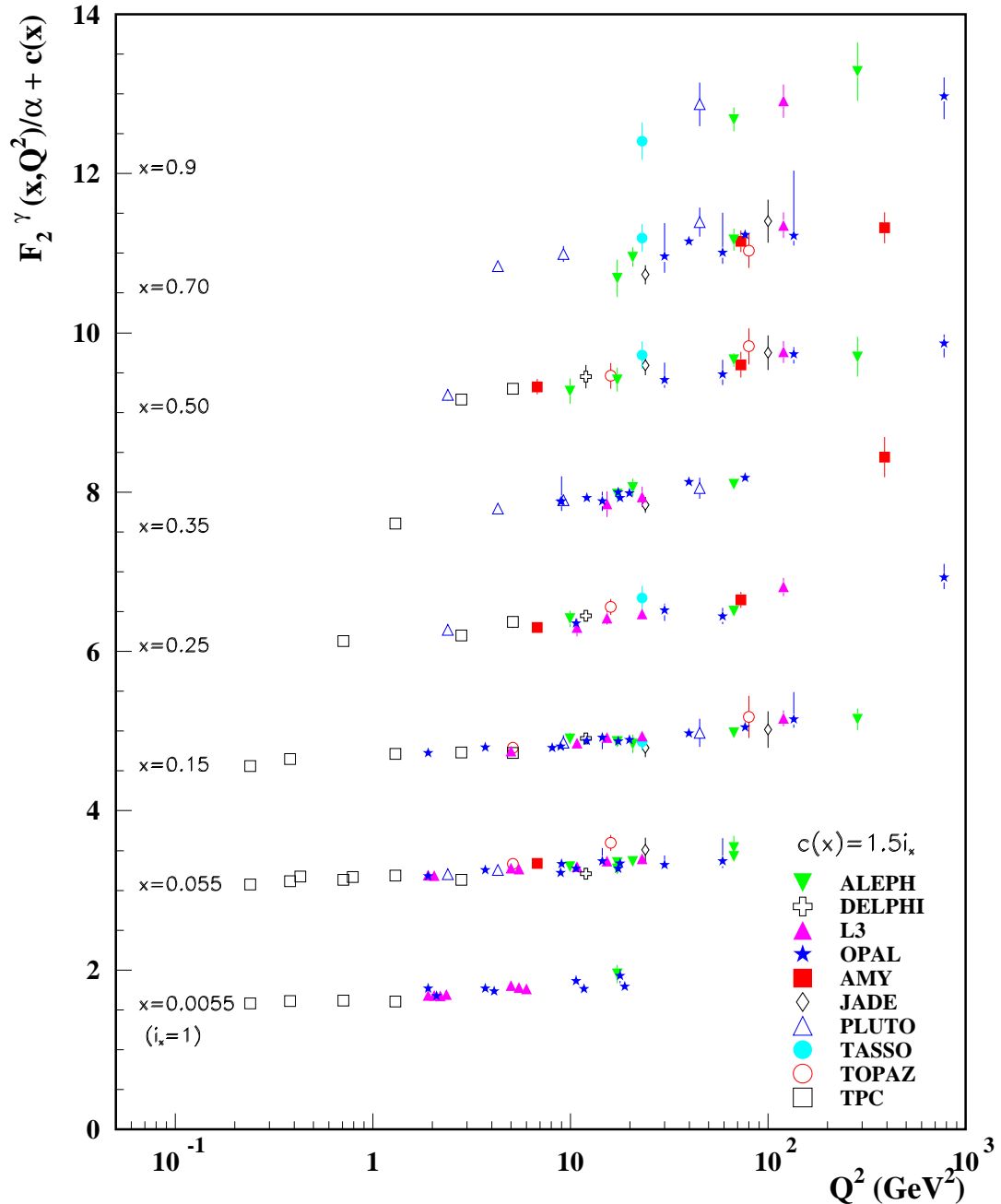


Figure 18.15: The hadronic structure function of the photon F_2^γ divided by the fine structure constant α measured in e^+e^- scattering, shown as a function of Q^2 for bins of x . Data points have been shifted to the nearest corresponding x bin as given in the plot. Some points have been offset in Q^2 for clarity. Statistical and systematic errors added in quadrature are shown. For the purpose of plotting, a constant $c(x) = 1.5i_x$ is added to F_2^γ/α where i_x is the number of the x bin, ranging from 1 ($x = 0.0055$) to 8 ($x = 0.9$). References: **ALEPH**–R. Barate *et al.*, Phys. Lett. **B458**, 152 (1999); A. Heister *et al.*, Eur. Phys. J. **C30**, 145 (2003); **DELPHI**–P. Abreu *et al.*, Z. Phys. **C69**, 223 (1995); **L3**–M. Acciarri *et al.*, Phys. Lett. **B436**, 403 (1998); M. Acciarri *et al.*, Phys. Lett. **B447**, 147 (1999); M. Acciarri *et al.*, Phys. Lett. **B483**, 373 (2000); **OPAL**–A. Ackerstaff *et al.*, Phys. Lett. **B411**, 387 (1997); A. Ackerstaff *et al.*, Z. Phys. **C74**, 33 (1997); G. Abbiendi *et al.*, Eur. Phys. J. **C18**, 15 (2000); G. Abbiendi *et al.*, Phys. Lett. **B533**, 207 (2002) (note that there is overlap of the data samples in these last two papers); **AMY**–S.K. Sahu *et al.*, Phys. Lett. **B346**, 208 (1995); T. Kojima *et al.*, Phys. Lett. **B400**, 395 (1997); **JADE**–W. Bartel *et al.*, Z. Phys. **C24**, 231 (1984); **PLUTO**–C. Berger *et al.*, Phys. Lett. **142B**, 111 (1984); C. Berger *et al.*, Nucl. Phys. **B281**, 365 (1987); **TASSO**–M. Althoff *et al.*, Z. Phys. **C31**, 527 (1986); **TOPAZ**–K. Muramatsu *et al.*, Phys. Lett. **B332**, 477 (1994); **TPC/Two Gamma**–H. Aihara *et al.*, Z. Phys. **C34**, 1 (1987).